

Validation of the Simulation of Collision Events at the LHC

Peter Mättig
Universität Bonn

November 10, 2021

Contents

1	What Particle Physics is about: Example LHC	2
1.1	The status of the Standard Model	2
1.2	The forefront Experiment: LHC	3
2	Data Analysis and the Use of Simulations	4
2.1	From Data to Physics	4
2.2	The Role of Simulation for Data Analysis	4
3	Modeling the LHC processes	5
3.1	The Matrix Element of the Hard Collision	5
3.2	Parton Distribution Functions: Dressing the Initial State	6
3.3	Dressing of the Outgoing Partons	6
4	Detector Simulation	7
5	Principles of Validation and Uncertainties	9
5.1	Factorization of Migration	10
5.2	Is Factorization correct?	10
6	General Procedures of Validation in Particle Physics	11
7	Validation of the Physics Generators	11
7.1	pdfs	12
7.2	Pile Up in pp Scattering	13
8	Validation of Detector Simulation	15
8.1	Testing the Detector Geometry	15
8.2	Validation of Electron Simulation	15
9	How Simulation is applied in Data Analysis	16
9.1	Measurement of the Higgs Cross Section	17
9.2	Search for a Stop Quark	18
10	Discussion	20
11	Summary and Conclusion	21

Abstract

The procedures of validating simulation of particle physics events at the LHC are summarized. Because of the strongly fluctuating particle content of LHC events and detector interactions, particle based Monte Carlo methods are an indispensable tool for data analysis. Simulation in particle physics is founded on factorization and thus its global validation can be realized by validating each individual step in the simulation. This can be accomplished by adopting results of previous measurements, in - situ studies and models. Important in particle physics is to quantify how well simulation is validated such that a systematic uncertainty can be assigned to a measurement. The simulation is tested for a wide range of processes and agrees with data within the assigned uncertainties.

1 What Particle Physics is about: Example LHC

During the 1960's and 70's the then differing concepts of electromagnetic, weak and strong interactions were put on a common ground leading to a theoretical framework, the Standard Model (SM) [1]. It is based on Quantum Field Theory and is arguably the most encompassing and precisely tested theory of nature ever. It accommodates all measurements in an energy range of several 100 GeV¹ with just a few fundamental particles, which can be classified in three sectors

- Twelve spin 1/2 particles (fermions) that can be separated in quarks and leptons are interpreted as 'matter' particles.
- Three kinds of spin 1 particles (vector bosons), the photon (γ), the W , Z^0 , and gluons, that transmit the electromagnetic, weak and strong interactions of the matter particles, respectively.
- One spin 0 particle (scalar boson), the Higgs boson, to generate the masses of the fermions, force carriers and itself.

The SM predicts the complete dynamics of these particles based on 19 free parameters². These elements and concepts appear to be the basis for nucleons, atoms and eventually all phenomena beyond and are crucial for our current understanding of cosmology.

1.1 The status of the Standard Model

The development of the conceptual framework was followed by an intensive experimental and theoretical program to establish the existence of all SM components, measure the free parameters [2] and test their dynamical properties. All components of the SM have been observed, the last one, the Higgs boson, has been found in 2012 at the Large Hadron Collider (LHC) [3] of the European Center for Particle Physics (CERN, Geneva), and almost all allowed interactions have been confirmed. The free parameters are measured to very high precision, e.g. the values of the coupling strength of the strong interaction and the mass of the Z^0 , which will be used later, are determined as

$$\alpha_s(M_Z) = 0.1181 \pm 0.0011, \quad M_Z = 91.1876 \pm 0.0021 \text{ GeV} \quad (1)$$

i.e. they are known to the 10^{-2} and 10^{-5} level, respectively. Furthermore, despite intensive searches, no effect has been observed at accelerators that does not agree with the SM. Therefore physicists consider the SM as being confirmed as a theory for an energy scale of

¹Using quantum mechanical relations this energy range can be interpreted as 10^{-18} m, i.e. about 100 million times smaller than an atom

²The number increases if the masses of the neutrinos are considered. Not all of the parameters related to neutrinos have been measured. Since they do not affect physics at the LHC, the subject of this paper, they will not be considered further.

up to several 100 GeV. The SM is also internally consistent, i.e. void of any infinities even at energies many orders of magnitude beyond what can be probed in any foreseeable future.

Still, there is a reluctance to accept the SM as a final theory. For one, the number and pattern of its particles and parameters are unexplained. In addition the SM does not contain gravity, which, however, should only become relevant at $M_{\text{Planck}} = 10^{19}$ GeV, and it is not able to explain astrophysical observations like the existence of Dark Matter [4] and Dark Energy [5]. To address these issues, models have been devised that lead to physics beyond the SM (BSM). Searches for BSM physics have so far been futile, but they have moved more and more into the focus of experimental and theoretical activities.

1.2 The forefront Experiment: LHC

Searches for BSM physics require higher precision on SM processes and in particular higher energies. The energy frontier of particle physics is the LHC, where every 25 nano - seconds a bunch of 10^{11} protons crosses another bunch flying in the opposite direction. Currently each of the protons has an energy of 6.5 TeV leading to the highest collision energies reached in an accelerator and a huge rate of collisions. Protons are composed of subcomponents, quarks or gluons, denoted together as partons. At the LHC the protons serve only as vehicles for the partons and high energetic parton collisions are of the main interest. They produce a large variety of very different physics processes.

Each LHC bunch crossing leads to 'an event' consisting of a spray of some 1000 particles, which are recorded by highly precise and sophisticated detectors covering almost the whole solid space angle and organized in different components. Their electronic recordings are translated into 'physics objects', i.e. candidates for electrons, quarks, photons etc. - each one a stable SM particles. The content of an event, i.e. how many of these different objects are found and their relation, e.g. relative angle or mass, make up the 'event signature'.

In this article the ATLAS experiment [6] will be considered³. It extends 40 m along the beam line and has a diameter of 25m in the transverse plane. Each of its components is sensitive to a particular type of particle, offering redundant and rather comprehensive information. The wide coverage of the particles from the interaction allows ATLAS to probe almost all of the LHC physics. In a sense ATLAS combines some 100 distinct experiments of previous times. This allows it to make optimal use of each event including cross calibrations, an essential point for the validation of the simulation - as will be discussed later.

The large number and variety of particles in each event reflect the statistical properties of quantum mechanics. The main experimental challenge is to infer the underlying parton scattering from the different event signatures. It is at this point that simulation as a tool for data analysis enters the field. Describing the large number of particles, their complicated and statistically distributed structure, as well as the statistical nature of their interactions in the detector cannot be achieved analytically but requires numerical methods.

The article will start with a short overview over the principles of data analysis and the use of simulations in particle physics, it will then discuss the two basic ingredients that enter simulation, the modeling of the physics process and that of the detector. It will then formalize the principles of simulation to motivate validation procedures in particle physics before discussing examples of validation in some detail and how simulation and validation works in typical analyses. Finally some points raised in the philosophical literature on simulations are commented.

³ The simulation for other LHC experiments CMS [7] and the specialized experiments ALICE [8] and LHCb [9] work along fairly similar principles.

2 Data Analysis and the Use of Simulations

Before describing the validation process in more detail in Sect. 5, we will summarize the ingredients of the simulation in particle physics. The simulation is particle based, involving a wide range of different scales and is realized with computer codes applying Monte Carlo (MC) methods.

2.1 From Data to Physics

The principal aim of the simulation of LHC events is to understand how the physics process ('signal', S) of interest would look in the detector. Comparing the measurement with this expectation allows one to extract information about the physics process of interest, e.g. a parameter of the SM, dynamic properties, or evidence, respectively exclusion of BSM effects.

Each S has a certain event signature. However, such signature is not unique but can also be due to competing processes, the 'background B '. To reach high sensitivity analyses aim at a good S/B ratio by applying special selections exploiting different properties of the S and the B processes. Arriving at a physics conclusion from the data requires the measurement to be compared to theory and thus to simulate both S and B .

In this article basic concepts of validation will often be discussed along the production of a Higgs (h), and the detection via Z^0 bosons and electrons⁴.

$$g + g \rightarrow h \rightarrow Z^0 Z^{0*} \rightarrow (e^+ e^-)(e^+ e^-) \quad (2)$$

i.e. two gluons g produce a Higgs that decays into two Z^0 bosons⁵, each of which then decays into pairs of electrons. The Higgs signal competes with background processes that also lead to four electrons but have no relation to Higgs production.

A key observable for the Higgs production and decay, but also of general importance, is the cross section σ_S , essentially a measure of the production yield. The cross section of a signal process is obtained from the measurement by

$$\sigma_S = \frac{N_{\text{sel}} - N_B}{\mathcal{L} \cdot \epsilon_S} \quad (3)$$

where \mathcal{L} is the luminosity, the total number of all possible proton - proton collisions provided by the LHC, N_{sel} is the number of data events, i.e. with four electrons, that have been selected, N_B , the number of background events and ϵ , the efficiency to detect a selected signal event, i.e.

$$\epsilon_S = \frac{N_{\text{sel}}^S}{N_{\text{prod}}^S} \quad (4)$$

where N_{sel}^S , N_{prod}^S are the numbers of signal events that are selected, respectively, produced.

2.2 The Role of Simulation for Data Analysis

Both N_B and ϵ are obtained from simulation and should be determined to a high precision. Per year some 10 trillion events are simulated for ATLAS, each taking several minutes. To make this work 100000 CPUs and 100s of petabytes of disk storage are provided by a world wide computing grid. To guarantee a constant quality, the simulation is continuously checked with bench mark processes.

Simulations in particle physics are used for several purposes.

⁴For simplicity particles and anti-particles will just be denoted by the name of the particle.

⁵The notation Z^{0*} means that the boson is 'off shell', i.e. its mass is different from the default 91 GeV due to quantum mechanical uncertainty.

- In the data analysis they are instrumental to obtain model predictions and their experimental signatures that can be compared to measurements.

This is the broadest and most challenging application that will be primarily considered in this article. In addition simulation is used to optimize tools and strategies.

- Both in experimental and theoretical studies simulation is used to evaluate the feasibility of a technique.
- Simulations are used to optimize the lay - out of future detectors, or detector conditions to run an experiment.

In all three use cases simulation is an auxiliary method to experiments, but in no way replaces measurements with real experiments. E.g. even if a detector component is first devised with simulation, it is only after studying an actual prototype, that the component will be integrated into the experiment. Simulations allow complicated manipulations of fairly involved models. Their results are believable only to the extent that the input and structure of simulations is believable, which in turn requires the input to and the structure of simulation to agree with experimental data. I.e. validation of the simulation is essential.

In particle physics, two main parts have to be simulated, the underlying physics processes leading to a distribution of hadrons, photons and leptons, which can be measured in the detector, and the detector response to each of these particles. Both parts will be introduced in turn in the subsequent sections.

3 Modeling the LHC processes

A general LHC collision of two partons A , B producing a signal S , which decays into two particles C , D , can be written as

$$A + B \rightarrow S \rightarrow C + D \quad (5)$$

A characterizing parameter for the parton collisions is the hardness of a collision Q^2 , which is given generically by $Q^2 = (p_C - p_A)^2$. Here $p_i = (E_i, \mathbf{p}_i)$ are the four momenta of the particles, with E the energy and \mathbf{p}_i the momentum components in the three space directions. 'Soft collisions' have a Q^2 of a few GeV^2 , hard collisions at the LHC are typically $(100 - 1000 \text{ GeV})^2$.

The outgoing electrons of Eq. 2 are rather easy to simulate. More complicated are reactions where also the final state particles C , D are strongly interacting partons. Due to the specific properties of the strong interactions, these partons cannot be observed directly, but are 'dressed' by many additional partons at distances smaller than 10^{-15} m. In the detector hard partons appear as narrow cones of some 20 - 40 particles, deemed 'jets'. A jet event recorded with the ATLAS detector is shown in Fig. 1 To understand this dressing is important to infer from the measurement on the initial parton collision. It is modeled based on the precisely probed theory of strong interactions (Quantum Chromo Dynamics, QCD) and simulated starting from the high Q^2 parton collision Eq. 5 to low Q^2 , where QCD inspired models⁶ of parton emissions are invoked. These models are not unambiguous and several variants exist, all being cast into computer codes using Monte - Carlo methods. We will now provide more details on the individual steps.

3.1 The Matrix Element of the Hard Collision

The fundamental differential equation for the process Eq. 5 is known, but cannot be solved in a closed form. Instead it is perturbatively expanded in the strong coupling $\alpha_s(Q^2)$ leading

⁶Here the particle physicists' notion of 'model' is used, which refers to a theoretical description of a physics process that is not fully calculable from the well founded and established 'theory' of the Standard Model.

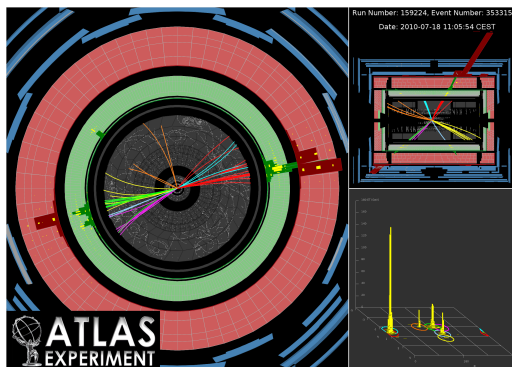


Figure 1: Two - jets event recorded at the LHC. The different components of the ATLAS detector are shown in the plane perpendicular to the beam direction (left), along the beam (upper right) and in the plane of polar and azimuthal angles (lower right). The tracks in the inner detector and the energy deposition in the calorimeters are indicated and show that energy is collimated in a rather small region, i.e. shows 'jetty' behaviour. [10]

to quantum mechanical matrix elements, which can be solved exactly. Schematically this can be written as (see eg. [11])

$$\sigma(A+B \rightarrow S) = \sigma_0(A+B \rightarrow S) + \alpha_s \sigma_1(A+B \rightarrow S) + \alpha_s^2 \sigma_2(A+B \rightarrow S) + \dots \quad (6)$$

where α_s is given by Eq. 1. The higher the order in α_s , the more complex is the calculation, but since α_s is of order 0.1 its contribution also becomes smaller. The complete perturbation series cannot be determined and is instead truncated, for LHC processes typically at the α_s^2 term. I.e. small contributions to the full cross - section are missing.

3.2 Parton Distribution Functions: Dressing the Initial State

Since the partons A , B in the initial state are subcomponents of protons they assume just a fraction of the proton energy p , parametrized as

$$x(\text{parton}) = \frac{p(\text{parton})}{p(\text{proton})} \quad \text{for } p(\text{proton}) \rightarrow \infty \quad (7)$$

x follows a probability distribution denoted as 'parton distribution function (pdf)', and enters the prediction of a cross section but cannot be calculated. The Q^2 dependence of the pdfs is, however, given by theory and has been experimentally well confirmed (see Sect. 7.1).

3.3 Dressing of the Outgoing Partons

To dress the outgoing partons C , D into jets, QCD based models are invoked, in which each final parton of the matrix element calculation is assumed to branch into further partons, which subsequently branch again.

The models follows each parton individually neglecting quantum mechanical interferences. Each of these branchings happens at some Q^2 , which decreases with the order of the branching. Since $Q \sim 1/t$ (t denoting time), this parton showering can be interpreted as a time ordered (Markov) chain. Modeling particle production in jets can be classified into three steps (for more details see [11, 12]).

1. The scattered partons C , D split into more partons, a so - called 'parton shower'. How the energy of a single parton is split among its daughters follows directly from theory.

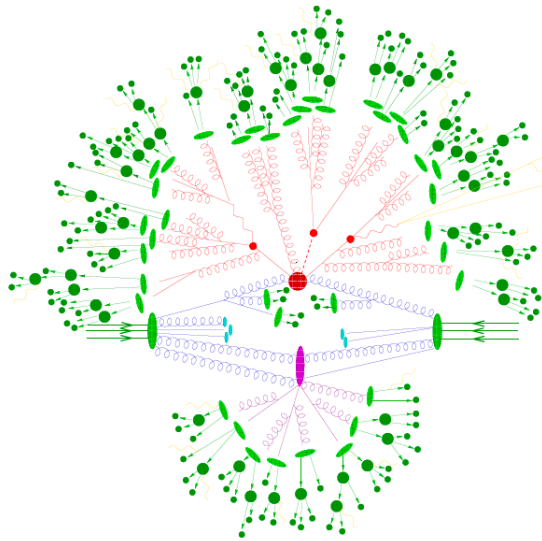


Figure 2: Schematic LHC event: straight lines denote quarks, curly lines gluons. The initial partons make a hard collisions (denoted by the large red circle) and split into other partons. Four immediately outgoing partons are shown, one (dashed line) decays only after flying a small distance. These partons branch further with increasingly smaller energy and angle resulting in jet like structures. Finally these partons turn into hadrons (shown as green lines/dots). In parallel the other partons inside the protons also interact (elongated pink area) leading to hadrons. [13]

2. These partons are finally turned into stable hadrons making up 'jets'. The details of this 'hadronization' are condensed in 'hadronization functions' expressing the probability of the energy and the kind of hadron to be produced. They are provided using previous measurements.
3. Whereas in the hard process just one of the many partons inside each proton interacts, the remnant ones also produce a spray of particles. This 'underlying event' is measured using special LHC processes.

This means that jet evolution can be simulated with a Markov chain by describing individual steps with special probability distributions. A rather complicated particle structure emerges, as schematically depicted in Fig. 2, where the many and diverse parton branchings become apparent, motivating the use of Monte - Carlo simulation.

Events at the LHC are further complicated by the occurrence of hadrons from additional pp collisions in the same LHC bunches. These contribute a 'pedestal' of particles to the hard collision of interest and are denoted as 'pile - up' events. These can be determined from data (see Sect. 7.2).

4 Detector Simulation

The modeling of the physics process terminates with a list of stable particles: hadrons, photons, electrons, muons and neutrinos. These are relevant for what is seen in the detector. Apart from neutrinos all particles interact with the detector material and generate electronic signals. Roughly speaking, as becomes apparent in Fig. 3, each of the components of the ATLAS detector has a special sensitivity to one of these particles. Their reconstruction provides a picture of what has happened at the collision point.

The principle of detector simulation is that each stable particle is traced inside the detector up to a volume element containing some material. They may interact according to probabilities obtained from models. The products of the interactions are then further

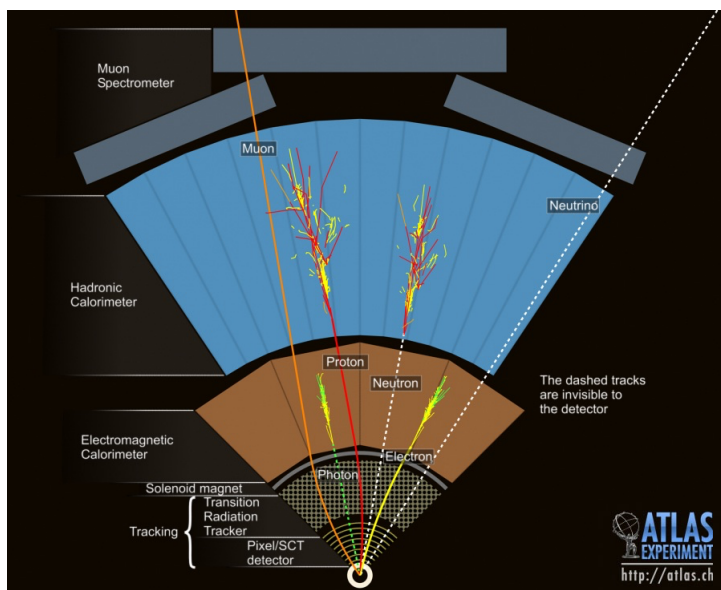


Figure 3: Schematics of the interactions of various types of stable particles in the components of a typical LHC detectors. As becomes apparent by combining the information the particle type can be identified [14]

traced to the next volume element with material and so on⁷. All material affects the passage of a particle and has to be considered, but only part is 'active' meaning that it generates electronic signals that are used to reconstruct the event.

These interactions and generated signals are cast into computer codes [16] that have been developed over the last 30 - 40 years and applied and validated in various, rather different detector environments. The main ingredients of these simulations are

- the geometry and materials of the detector,
- methods of numerical integration to follow a particle, partly inside a magnetic field,
- modeling the particle interactions in the material.

The detector geometry is mapped in a first step according to engineering drawings that have been used for building the detector. When relevant, one includes fine details, in part as small as several μm^3 , as can be seen from Fig. 4(left) showing schematically one of the 80,000 modules of the pixel detector, the innermost component of ATLAS. The interactions with the material are simulated stochastically using the interaction cross section of the incoming particle h with the material A under consideration. i.e.

$$\sigma_{\text{int}}(h + A) = \sigma_1(f_1) + \sigma_2(f_2) + \dots \quad (8)$$

where the f_i are possible final states, which may consist of several particles. The respective momenta are generated according to models cast into computer codes, e.g. [17, 18]. Those for incoming electrons and photons are rather well understood, interactions of hadrons are more uncertain.

The interactions in the active volume will then be digitized, i.e. translated into an electronic signal.

While the simulation should be as precise as possible, it is not meaningful to exceed the measurement uncertainty and also it should be balanced with the required computing time. Therefore some effects are integrated over and condensed into a single parameter.

⁷For a more detailed and also historical account of detector simulation in particle physics see [15].

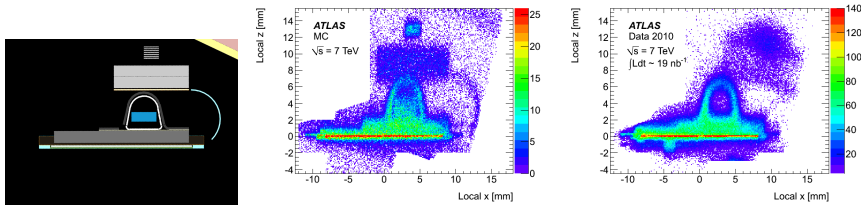


Figure 4: Display of a component of the ATLAS pixel detector. The total length of the object is 2cm, the widths of individual parts are as small 0.02 mm. (a) The distribution of the material in the simulation [14], (b) the material in the simulation as seen in interactions of particles, (c) the material as seen in real collision events. Red indicates many interactions, blue relatively few [19].

The simulation of the pixel detector is an example of the balance between fine details and required precision. There an electronic signal is caused by some 30,000 electron - hole pairs that are produced from the passage of a particle through a 250 μm thick silicon layer. It is well understood how these pairs are produced and move towards the electrodes, thus simulating these would be possible. However, such detailed simulation is only meaningful if supplemented with a simulation of each of the somewhat different 80,000 electronic circuits, requiring an excessive use of computing resources. Instead the response of the pixel detector to particles is measured and the probability distribution of the signal depending on the particle's properties is used in the simulation without considering the details of its generation. No uncertainty is induced by this discretization.

As a side remark, one should be aware of the hugely different scales in detector simulation. Within a detector of a global diameter of 25 m, structures of the size of 0.00001 m are considered, if important. How finely the volume elements in the simulation are granulated, depends on their impact on the measurement and has been tested.

The simulated electronic signals in the various parts of the detector are then subjected to the identical procedure as the recorded data to reconstruct physics objects, i.e. electrons, muons, jets etc..

5 Principles of Validation and Uncertainties

Formally simulation in particle physics translates an original, 'true' distribution T of partons C, D with energy $E_{C,D}$, 3 - momenta $\mathbf{p}_{C,D}$ and types $f_{C,D}$ into n reconstructed particles with respective energies, 3 - momenta and types, i.e.

$$\begin{pmatrix} E_1 \\ \mathbf{p}_1 \\ f_1 \\ E_2 \\ \mathbf{p}_2 \\ f_2 \\ \dots \\ \dots \\ E_n \\ \mathbf{p}_n \\ f_n \end{pmatrix} = \mathcal{M} \times \begin{pmatrix} E_C \\ \mathbf{p}_C \\ f_C \\ E_D \\ \mathbf{p}_D \\ f_D \end{pmatrix} \quad (9)$$

where n is $\mathcal{O}(1000 - 100000)$. The transformation \mathcal{M} expresses what is happening in the simulation. Instead of listing all momenta of individual particles, the main idea can be visualized in a simpler way by considering some distribution z of (physics) interest, e.g. the mass M of an event.

Along the discussion of Sect. 3.1, the matrix element calculation in some model yields the 'true' mass distribution $T(M_{C,D})$. In simulation the C , D are dressed and affected by experimental resolutions such that $T(M_{C,D})$ is transformed into a prediction $P(M)$ for the mass distribution that is supposed to be measured for the model under consideration. Actually measured in the experiment would be a distribution $D(M)$. To interpret the measurement, e.g. to infer on the validity of the model, $P(M)$ has to be compared to $D(M)$.

5.1 Factorization of Migration

In terms of z simulation means

$$P(z) = \mathcal{M}T(z) \quad (10)$$

Discretizing z in intervals the transformation can be expressed by a square matrix of the migration of a theoretical mass value to an observed one.

$$\mathcal{M} = \mathbf{m}_{ij} = \begin{pmatrix} m_{11} & m_{12} & \dots & m_{1n} \\ m_{21} & m_{22} & \dots & m_{2n} \\ \dots & \dots & \dots & \dots \\ m_{n1} & m_{n2} & \dots & m_{nn} \end{pmatrix} \quad (11)$$

where each element in the matrix relates a value of M in the incoming step to a mass of the outgoing steps. E.g m_{2n} is the probability that an event with a true z in bin n has a reconstructed z in bin 2. In the previous section it was discussed that simulation proceeds in (time - ordered) steps. Using the formalism each step corresponds to a special migration matrix \mathcal{M}_α . Here α denotes the effect under consideration, e.g. $\alpha = 1$ the effect of the pdfs, $\alpha = 3$ the one due to hadronization, $\alpha = k$ is the distortion from a detector component etc.. The complete simulation \mathcal{M} is then factorized into \mathcal{M}_α ,

$$\mathcal{M} = [\mathcal{M}_k \times \dots \times \mathcal{M}_2 \times \mathcal{M}_1] \quad (12)$$

$$P(z) = [\mathcal{M}_k \times \dots \times \mathcal{M}_2 \times \mathcal{M}_1] \times T(z) \quad (13)$$

More precisely, adding pile up $U(z)$ and background processes $B(z)$ to the signal process $S(z)$, one arrives at modified (primed) results.

$$T(z) \rightarrow T'(z) = (S + U)(z) + (B + U)(z) \quad (14)$$

$$P'(z) = \mathcal{M} \cdot [(S + U)(z) + (B + U)(z)] \quad (15)$$

The physics question is whether $P'(z) = D(z)$, which means S is correct, if \mathcal{M} , $U(z)$ and $B(z)$ are correct, but can also be fulfilled if e.g. S and \mathcal{M} are incorrect. Inferring on S from D requires one to validate \mathcal{M} and the background distributions.

5.2 Is Factorization correct?

These considerations, which will be crucial for the validation procedure discussed in the next sections, depend on factorization. It is evidently fulfilled if the steps are incoherent and follow a time sequence. This is clearly true for the detector simulation, where a particle from the pp interaction first interacts in the tracking detector before entering the calorimeter etc.. I.e. only those particles have to be considered in the simulation of the calorimeter response that leave the tracking detector (cp. Fig. 3).

The time - sequence in the transition from the matrix element to the final hadrons in the physics generator, however, is only approximate since quantum level interferences are left out. However, the factorization assumption is justified from theoretical arguments (e.g. [11])

at least for pdfs to rather high precision. The basic argument is that the different steps occur at significantly different energy scales, which hardly influence each other. Similar arguments for the validity of factorization can be applied to the showering and hadronization effects. In addition the assumption has been tested by comparing processes involving electroweak particles⁸.

6 General Procedures of Validation in Particle Physics

At face value data and simulation agree for SM processes at the LHC to stunning precision. In so far, the requirement in the philosophical literature, 'validation is said to be the process of determining whether the chosen model is a good enough representation of the realworld system for the purpose of the simulation' [20] seems to be fulfilled. However, as outlined above, the agreement is a necessary, but not a sufficient condition to claim the correctness of the model of the underlying parton process. Instead the migration matrix \mathcal{M} and the backgrounds have to be validated. The principle validation methods will be discussed in the next sections. The basic ideas are as follows.

1. For each \mathcal{M}_α the corresponding model is validated by either data from previous experiments, possibly together with a well founded theory, or better even, by an in-situ experimental validation. For this, dedicated processes are used, each isolating a specific effect. If all steps of the simulation are validated then, obviously, the whole simulation is validated and the sufficient condition is fulfilled to infer from the agreement of simulation and data on the underlying physics process. All steps means that both the underlying physics model, which is a genuine part of the simulation, and the description of the detector response have to be validated
2. Given that simulation should help to provide quantitative statements on SM parameters or BSM effects, validation should provide an estimate of how well a process is validated. This is expressed as a 'systematic' uncertainty for each validation step $\delta(\mathcal{M}_\alpha)$. In this sense the process of validation is synonymous with the process of assigning an uncertainty. By error propagation this leads to a total uncertainty $\delta(P'(x))$ of the simulation prediction.

It is beyond the scope of this article to cover the complete validation procedure, which is documented in numerous publications and notes (some will be mentioned in the text). Instead some examples will be presented in more detail, highlighting general methods used in the validation of both physics and detector modeling

- a combination of previous experiments and model assumptions,
- measurements of LHC processes that are complementary to the process of interest,
- in-situ measurements of properties of the detector,
- adjusting the simulation to data using previous precision measurements.

As will hopefully become apparent in the following sections, the different 'factors' that enter simulation at the LHC are experimentally tested and simulation is applied on a significantly constrained material basis. This discussion, although maybe sometimes technical, seems to be important in view of claims that 'in the context of the LHC there is a lack of experimental data for comparison [with simulated data]' [21](290).

7 Validation of the Physics Generators

The parton distributions in a space - time region of smaller 10^{-15} m and the model of how they turn into hadrons, have been discussed in Sect.3. These processes are statistically

⁸I.e comparing a W decay in $e\nu$ with those in $q\bar{q}$ or production cross sections and jet structures in of $e^+e^- \rightarrow q\bar{q}$

distributed and thus a generic part of the computer simulation. Moreover, since the parton evolution is described by models, these have to be validated.

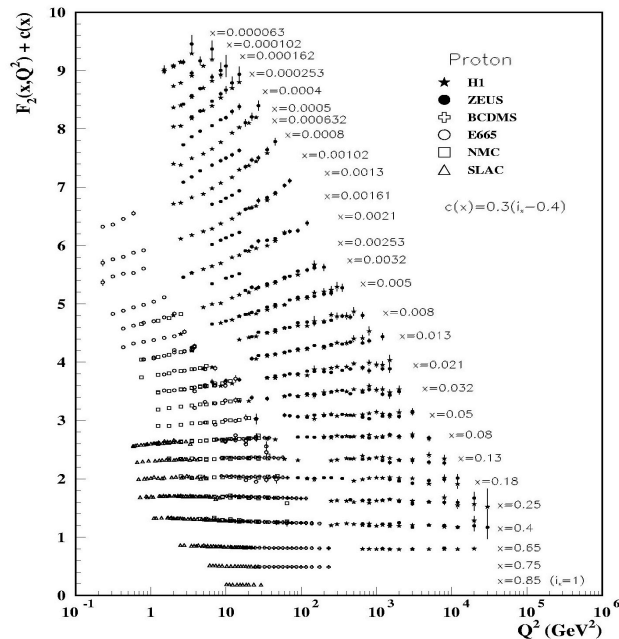


Figure 5: Measurements on the Q^2 dependence of the pdf. Shown are measurements from several experiments and in different bins of x [2].

As examples validation of pdfs and pile - up events will be discussed in the following sections. But before a brief comment on the other steps. As discussed, the perturbation series of the matrix element of the hard process are truncated. The magnitude of the remaining terms is estimated by a convention that has been tested in various processes such that uncertainties of typically some 3-5% are assigned. The basic understanding of the major other steps, i.e. showering and hadronization (see Sect. 3.3), has been obtained from previous experiments at e^+e^- colliders [22, 23] and cross - checked with LHC data (see e.g. [24]). The steps are described by various models, and their differing outcomes provide the uncertainty range assigned to showering effects.

7.1 pdfs

The pdfs are an essential ingredient of the simulation and instrumental for the interpretation of measurements. The cleanest way to measure pdfs is via the scattering of electrons on nucleons. A compilation of the major experiments is shown in Fig.5 for various intervals in x as a function of Q^2 . Whereas the pdfs themselves cannot be calculated from first principles, their Q^2 dependence is precisely known in QCD and excellently confirmed by measurements. Knowing the pdf at one Q^2 allows one to extrapolate it to another Q^2 (for more details see [25]).

Such extrapolations are needed for the LHC, for which much higher Q^2 can be reached. Validation of the LHC has to address the question: what variations of pdf models are allowed by data at low Q^2 ? Given the knowledge of the Q^2 dependence how large are the variations at LHC conditions? Are there ways to test pdfs directly at the LHC avoiding circularity?

The uncertainties of pdfs at a certain Q^2 are due to both measurement uncertainties and theoretical ones. The latter ones come e.g. from inter- and extrapolating the binned

measurements to a continuous distribution. Given the number of input bins there is in general only a small amount of variation allowed. However at the extremes like $x = 0, 1$, they can be important. These ambiguities lead to different pdf models with some variation in the expectations for the LHC, none of which can be a priori excluded.

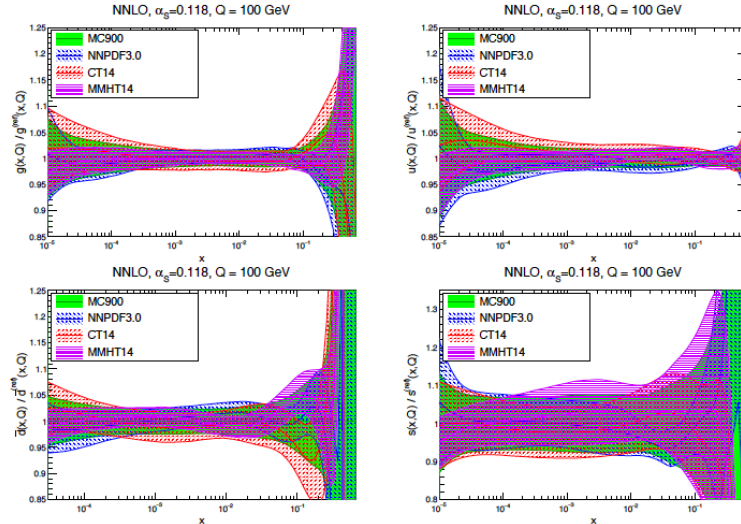


Figure 6: Predictions for the pdfs of gluons (upper left), up quarks (upper right), anti - down quarks (lower left) and strange quarks (lower right) are shown for $Q = 100$ GeV and an x range stretching over 5 orders of magnitude. The different colours correspond to different pdf models, all are shown being normalized to the average of these. The coloured bands correspond to the uncertainties assigned to the corresponding model. [26]

As an example, four different pdf models for different kinds of parton species at a $Q = 100$ GeV (i.e. close to the relevant scale for the Higgs production) are shown in Fig. 6. As can be observed, the difference between different models is in general smaller than the uncertainty assumed for an individual model - an indication that the constraints from data are fairly tight. The variation between these pdf models together with their individual uncertainties are used as an overall pdf uncertainty of typically below 10%. A notable exception are very high x values.

In addition, these predictions can be validated by using special LHC processes. Particularly those involving W and Z^0 production provide in situ constraints on pdfs [27]. In addition the energy dependence of the yields of theoretically well understood processes like the production of top quarks ($t\bar{t}$) can be used [28]. Both examples are depicted in Fig. 7. These cross checks show that the assumed pdf models derived from non - LHC experiments and their uncertainties are consistent with the LHC measurements.

In addition, these predictions can be validated by using special LHC processes. Particularly those involving W and Z^0 production provide in situ constraints on pdfs [27]. In addition the energy dependence of the yields of theoretically well understood processes like the production of top quarks ($t\bar{t}$) can be used [28]. Both examples are depicted in Fig. 7. These cross checks show that the assumed pdf models derived from non - LHC experiments and their uncertainties are consistent with the LHC measurements.

7.2 Pile Up in pp Scattering

As stated in 3.3, every hard interaction of interest is accompanied by some 30 additional and incoherent pp interactions in one bunch crossing, called pile - up. This 'pile - up' has to be an integral part of the simulation of a LHC event. Validation of these requires the

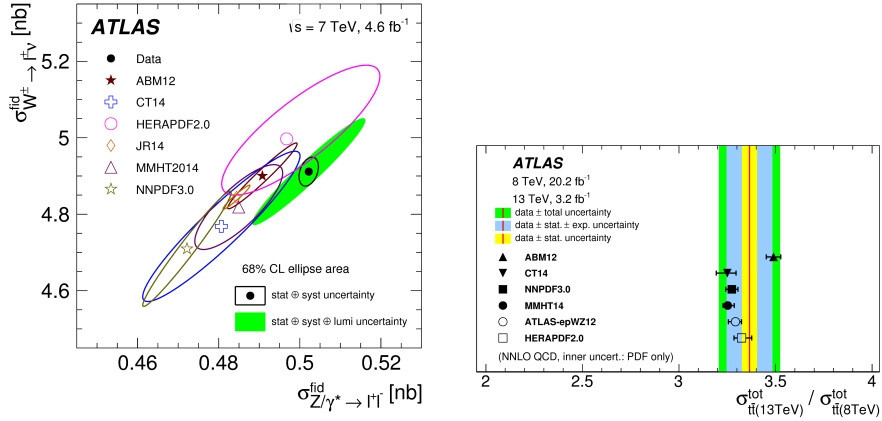


Figure 7: ATLAS Measurement of W^\pm vs. Z^0 (left), being sensitive sensitive to other quark species. The data are compared to the expectation from various pdf models. The ellipses indicate the corresponding uncertainties, i.e. the 66% certainty range. [27]. The right figure compares production of pairs of top quarks at two different LHC energies [28].

properties of these events to be understood. This is achieved by direct LHC measurements (e.g. [29]).

Since pile - up events have a high cross section at the LHC, they are frequently produced in bunch crossings, but can also be measured individually with short special LHC runs. Based on these measurements, QCD inspired models are devised to describe pile - up events. These models are then used in the simulation to overlay pile - up to the physics processes of interest.

Pile - up events are found to largely produce an isotropic spray of low energy particles as is apparent from the measurements shown in Fig. 8.. In the Figure data are compared to several models. As can be seen some of them describe the measurements rather well and are used in simulation. The remaining deviations between the preferred models and data are small and do not affect the measurement in any relevant way.

Pile up events can be seen as an example, where the large variety of LHC processes can be used to measure some process i directly as input to simulation for complementary physics processes j .

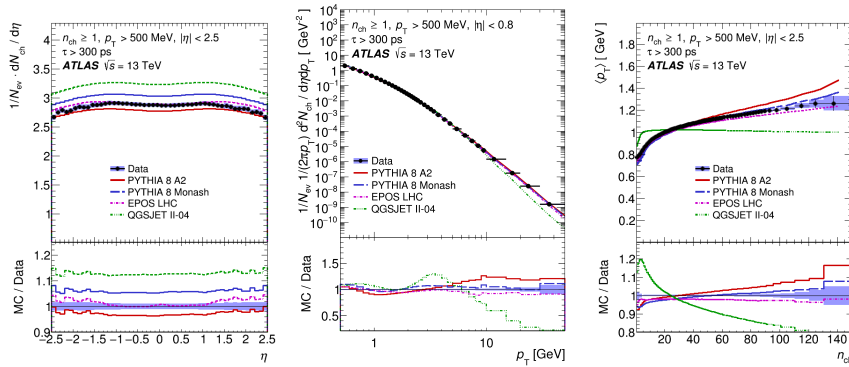


Figure 8: Relevant properties of one pile-up event as measured in low luminosity runs. The production angle wrt. the beam direction (left) and the transverse momentum p_T distribution of charged particles are shown (center) and the average event p_T as a function of the number of charged particles in an event (right) [29]

8 Validation of Detector Simulation

The modeling of the detector is crucial to understand how well particles can be reconstructed from electronic signals in the detector components (cp. Sect. 4). Here we focus on detector geometry and simulation of electron properties.

8.1 Testing the Detector Geometry

While the starting point for the description of a detector are engineering drawings, once the detector is installed details may change rendering the simulation inaccurate. As an example, consider a module of the pixel detector whose engineering drawing is shown in Fig. 4(left) and serves as a blueprint for the simulation. Data allow one to 'see' the material distribution with a tomography - like method.

The method is based on the number and position of particle interactions inside the detector⁹. Their frequency is a measure of the material. For a pixel module the number of interactions in a projected area of $100 \times 100 \mu\text{meter}^3$ is shown in Fig. 4(centre)[19]. The one-to-one correspondence with the input geometry clearly shows the method to work¹⁰.

The interesting step is to apply this tomography to data. The result is shown in Fig. 4(right). Whereas the general structure agrees well with the simulation, there are also important differences. E.g. the rectangular component in the simulation around $z \sim 10$ cm correspond to cables, which are much more spread out in the real detector, the circular shape around $x = 3$ cm is a cooling pipe. In the simulation it is considered to be mostly filled with a liquid, in the data it becomes apparent that most of it is in gaseous state. Furthermore at $x = -4$ cm an electronic component (capacitor) is visible in the data, which had been omitted in the simulation. After these differences became known, the simulation has been adjusted.

The details of this discussion are not important, but the message is that the geometry of the detector can largely be checked and corrected with the data themselves.

A variety of procedures are used for different components. They are examples of in - situ measurements based on well established types of reactions and redundancies in the detector.

8.2 Validation of Electron Simulation

A key particle for LHC physics is the electron, which is produced in many SM and perceived BSM processes and relatively easy to identify. Data analysis requires one to know the detection efficiency (cp. Eq. 4), the 'true' energy E_{true} and the energy resolution σ_E as given by

$$E_{\text{meas}} = (1 + \alpha) E_{\text{true}} \quad (16)$$

$$E_{\text{true}} \rightarrow f(E) \propto e^{(E - E_{\text{true}})^2 / 2\sigma_E^2} \quad (17)$$

where $1 + \alpha$ is the electron energy scale indicating a possible mismeasurement, and σ_E is a measure of how strongly the measurements fluctuate. Evidently it is crucial for the simulation to describe these appropriately.

Simulations of interactions of electrons with material are based on a well established theory, and have been studied numerous times and with many detectors, also in test - beams for the calorimeter components later installed in ATLAS. The electronic response in the calorimeter to the electron energy, however, needs to be calibrated. Given the precise knowledge of the Z^0 mass from previous measurements at the e^+e^- collider LEP [30], see

⁹These interactions in the detector are completely distinct from those pp interactions to test the SM and find BSM signals.

¹⁰This test of validation tools represents another use of simulation in particle physics, mentioned in Sect. 2.2

Eq. 1, and the abundant and clean Z^0 production at the LHC (see Fig. 9 (left) [31]), the electron energy is calibrated to reproduce the Z^0 mass. To take into account distortions of the shape of the Z^0 peak due to secondary interactions of the electron with the material in front of the calorimeter, this calibration is based on the Z^0 shape obtained from simulation.

Before this general procedure is realized, the simulation of the electron inside the calorimeter has to be validated in - situ. E.g. inhomogeneous material distributions are obtained from the longitudinal evolution of a shower, and modifications of the calorimeter geometry due to gravitational effects are derived from angular modulations of the ratio of redundant measurements in the tracking detector and the calorimeter. The observed deviations are taken into account by parametric corrections of the simulation [32].

Whereas the Z^0 mass has been measured and can serve as a reference, the energy resolution is detector specific. Still, the Z^0 serves as a marker for validation in that its observed width is a measure of σ_E . Differences between data and simulation are actually observed and the simulation is smeared to accommodate this discrepancy. The impact of this correction in the simulation can be seen in Fig. 9(right), where the ratio of data and simulation of m_{ee} is shown before and after the correction. Similarly the electron efficiency is determined by in-situ measurements of the Z^0 decay. The simulation is adjusted to agree with the data [33].

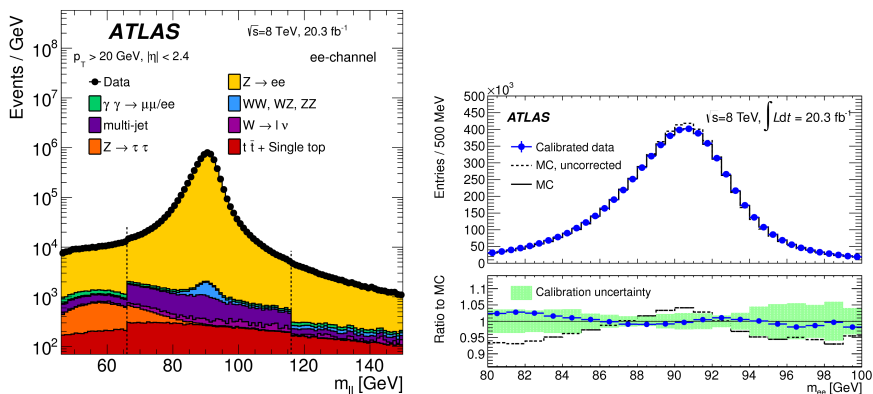


Figure 9: The e^+e^- mass distribution observed with the ATLAS detector (left) [31]. Also shown are the background contributions. Comparison of data and simulation before and after adjusting the simulation to the Z^0 peak as a function of the e^+e^- mass (right) [32]. The ratio between data and simulation is shown in the lower part.

I.e the simulation of electrons can be validated in - situ, making use of the redundancy of the detector, the wide range of LHC processes and in particular a highly precisely measured reference process. The high statistics and precise knowledge of the references also imply that the uncertainties assigned to simulation is small. Similar procedures also exist for other particles, e.g. [34, 35].

9 How Simulation is applied in Data Analysis

In this section two examples will be discussed of how simulation is applied in data analyses. These will also show methods to validate the background simulation. In the first example properties of a known particle, the Higgs boson, are determined in a kinematic region that is well probed. The second example is a search for a BSM effect which requires extrapolations into as yet unexplored energy regions.

9.1 Measurement of the Higgs Cross Section

In July 2012 both the ATLAS and the CMS collaborations announced the observation of a new particle with a mass of 125 GeV [36] through its decay into pairs of particles, especially into ZZ^* and $\gamma\gamma$. To establish if this is the long sought for Higgs boson, the properties of the particle had to be determined. One key measurement is the cross section (cp. Eq. 3) $\sigma_{h \rightarrow XX}$ for the Higgs production and its decay into two particles XX . Since the SM and alternative models for mass generation lead to different cross sections, their precise measurements can discriminate them. Here we will discuss $X = Z, Z^*$ along [38], with each Z decaying into a pair of electrons.

In Fig. 10 the observed mass distribution of the four leptons (either electrons or muons) from the ZZ^* decays is shown. An enhancement around 125 GeV can be seen over an almost flat background. How this signal is translated into $\sigma_{h \rightarrow ZZ^*}$, will be outlined assuming a pure electron signal, although in the analysis both electrons and muons are used.

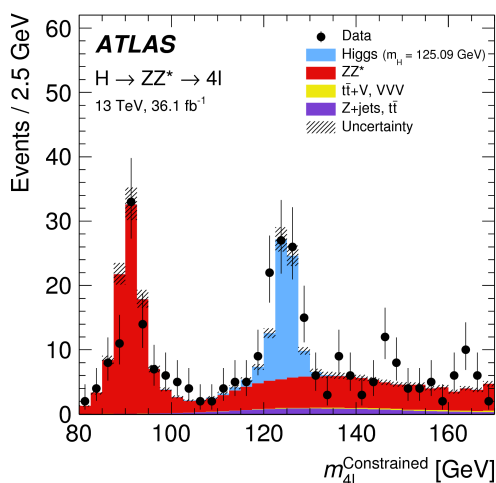


Figure 10: Spectrum of the four lepton mass consistent with a decay ZZ^* as measured by the ATLAS experiment [38]. The peak around 91 GeV is the Z^0 peak.

In a first step simulation is applied to find selections to reach a good signal to background ratio (S/B, cp. Sect.2.1). For the analysis events are selected that contain four electrons of which at least one has a minimum momentum p_T in the plane transverse to the beam direction of 20 GeV. All leptons should have an angle larger than 160 mrad wrt the beam axis. This defines the 'fiducial volume', in which the cross section is determined. Inspecting Eq. 3, one needs for the cross section measurement the efficiency and the background, i.e. the number of events that originate from other processes but also lead to four electrons.

The efficiency is affected by two major contributions. The first one is how many of the generated electrons are inside the fiducial volume. This is in a first step given by the matrix element, however, detector effects like the energy scale and resolution of electrons (see Sect. 8.2) have to be taken into account. The second is the detection efficiency of the electrons. Since the matrix element is known and the detector effects have been validated, the detection efficiency for $\sigma_{h \rightarrow XX}$ is obtained from Monte Carlo simulation by convoluting the physics model with the adjusted detector performance.

The dominant background source is continuum $Z^0 Z^*$ production, i.e. without an intermittent Higgs boson (see red area in Fig. 10), which tightly constrained outside the signal region around 125 GeV. Minor backgrounds are for e.g. due to top - pair production. These are estimated by a data driven method similar to the one that will be discussed in the next

section.

Relative to the theoretical expectation the measured cross section for a SM Higgs is

$$\left(\frac{\sigma(h \rightarrow 4l)_{\text{data}}}{\sigma(h \rightarrow 4l)_{\text{SM}}}\right)_{\text{fid}} = 1.28 \pm 0.18 \pm 0.07 \pm 0.07 \quad (18)$$

where the uncertainties are statistical, experimental systematic and theoretical, the latter including pdfs. The experimental systematic uncertainty corresponds to the uncertainty of the validation from simulation.

9.2 Search for a Stop Quark

A large fraction of the analyses at the LHC tries to find BSM signals. In this section it will be discussed, how simulation is applied in the search for supersymmetry, the most popular BSM model. The focus will be on methods to validate simulation of background processes.

More specifically, the search for the pair production of the supersymmetric partner of the top quark, denoted as stop (\tilde{t}), in the decay mode

$$pp \rightarrow \tilde{t}\tilde{t}^* \rightarrow t\bar{t}\chi^0\chi^0 \quad (19)$$

will be considered, where χ^0 is a particle that leaves no trace in any detector - and therefore is also a dark matter candidate. The production and decay properties of this process are rather precisely predicted such that the distribution of the outgoing partons can be reliably simulated. Here we assume a stop quark of high mass (of 1 TeV) and a massless χ^0 , following [39].

The experimental signatures of this process are a visible pair of SM top quarks ($t\bar{t}$), but in association with a very high imbalance of the detectable momentum in the plane transverse to the beam axis, caused by the two invisible χ^0 s. This is denoted as 'missing transverse energy', $E_{T,\text{miss}}$. One major background is due to two neutrinos from decays of top quarks,

$$pp \rightarrow t\bar{t} \rightarrow \nu\bar{\nu} + X \quad (20)$$

where X represents all other particles in the event. The validation of this process will be discussed here. Simulations are used to suggest a selection that leads to an optimal S/B ratio for stop production. This signal region (SR) is defined through six observables, of which the most important are

- $m_T > 160$ GeV, the mass of the lepton p_T and $E_{T,\text{miss}}$ system.
- $\text{am}_{T2} > 175$ GeV, a measure in how far the observed jets and leptons agree with coming from two stop quarks of mass 1 TeV¹¹.

The retained events are in kinematic regions, which have not yet been probed and are prone to possible misrepresentations of both Standard Model physics and detector modeling. Using the formalisms of Sect. 5.1, one can separate the whole distribution for simplicity into regions that have, respectively have not, been probed, i.e. $z < z_{\text{cut}}$ and $z > z_{\text{cut}} = (z_{\text{cut}} + \Delta)$. The z_{cut} may be identified with the selection requirement used to isolate stop pair - events and the region $(z_{\text{cut}} + \Delta)$ with the SR. In this region simulation of the Standard Model distributions is given by

$$P'(z_{\text{cut}} + \Delta) = [\mathcal{M} + \Delta\mathcal{M}] \cdot (B + U)(z_{\text{cut}} + \Delta) \quad (22)$$

¹¹The exact definition is

$$\text{am}_{T2} = \min_{\mathbf{q}_{T_a} + \mathbf{q}_{T_b} = E_{T,\text{miss}}} [\max(m_{T_a}, m_{T_b})] \quad (21)$$

I.e. the minimum parent mass consistent with the observed kinematic distributions assuming input masses m_{T_a} and m_{T_b} and certain mass combinations.

$\Delta\mathcal{M}$ represents the migration that has not been tested before, whereas $B(z_{\text{cut}} + \Delta)$ the Standard Model distribution in the not yet tested region.

It follows from Eq. 22 that the contribution to $P(z > z_{\text{cut}})$ is due to two sources: the Standard Model contribution $B(z > z_{\text{cut}})$ and the migration of events out of $B(z < z_{\text{cut}})$ (and of course both together). The simulation of the background yield, needs to be validated in the region $(z_{\text{cut}} + \Delta)$. This is done in two steps

- In a first step, a 'control region' (CR) for the process 20 is defined, which uses the same observables as the SR, with cut values in general as close as possible to the SR, but inverting the am_{T2} requirement. This enriches $t\bar{t}$ events, makes the SR and CR regions disjoint and the CR void of any signal. The normalized distributions (shapes) are sensitive to detector effects and data and simulation are compared for $z > z_{\text{cut}}$. As an example the m_T distribution is depicted in Fig. 11 (left) showing a good agreement. It underlines that the physics distributions and the detector effects are well described also for $m_T > 160$ GeV, which is sensitive to a potential stop particle. Once the shape is confirmed, the simulated cross section for $z > z_{\text{cut}}$ is scaled by¹².

$$r_{t\bar{t}} = \left(\frac{N_{\text{data}}(t\bar{t})}{N_{\text{simulation}}(t\bar{t})} \right)_{\text{CR}} = 1.01 \pm 0.15 \quad (23)$$

and therefore adjusted to the measurement.

- In a second step, a 'validation region' (VR) is defined where the selection is chosen to be in between the CR and the SR. A small, but negligible, fraction of events might come from the signal. Using the adjusted cross section for the simulation of the background, it is tested in how far the observed number and shape of events agrees with the expectation. Fig. 11 (right) shows that the data can be consistently described.

These studies validate the background distributions in the kinematic vicinity of the SR, but not in the SR itself. After having adjusted simulation to data in the CR and VR, one uses simulation to extrapolate. However, since these extrapolations depend on details of strong interactions (see Sect. 3.3), a range of QCD models is used to estimate its additional uncertainty taking into account the constraints from the CRs and VRs.

I.e. the background in the new region is estimated with methods which use simulation as guidance, but in the validation process they are adjusted to agree with the data. This procedure implies a significant uncertainty such that the search is sensitive only in regions where the S/B is high. In the stop analysis the expected number of Standard Model background events in the SR of 3.8 ± 1.0 , the uncertainty mostly due to the modeling uncertainties. The expected signal contribution from a stop would be 6. In the data 8 events are observed, i.e. more than expected from SM sources alone, but consistent with just a statistical fluctuation.

¹²Note that using this method, other backgrounds, like W +jets, show a visible discrepancy between simulation and data.

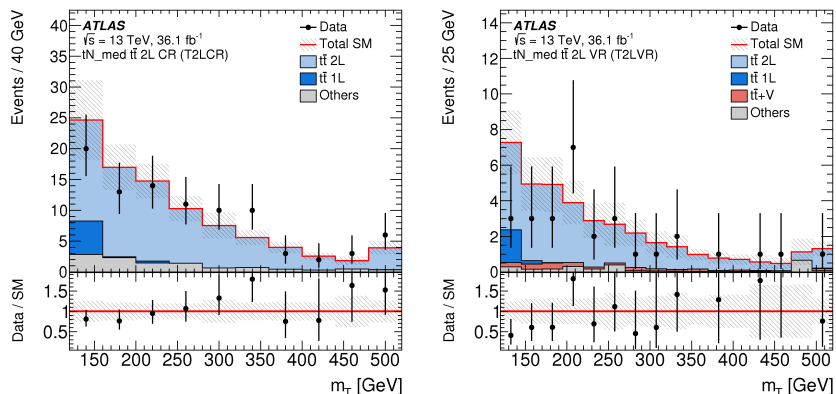


Figure 11: The m_T distribution for the control region (CR, left) and the validation region (VR, right). Shown are the expectations from the dominant Standard Model contributions from $t\bar{t}$ production and the data. The lower part shows the ratio data/simulated events [39].

10 Discussion

Simulation in science and its validation are debated in the philosophical literature from various perspectives. In this short section a few points are commented from the view of particle physics without being able to address them in detail.

Simulation of LHC events is characterized by the remoteness of the underlying physics and the complexity of the measurement device. As a result it involves hugely different scales. To say it strikingly, simulation covers the physics from distances of 10^{-18} meters to those of several meters in the detector. For the different scales specific models are employed, such that instead of one model a chain of models is used in simulation. This is the basis of factorization addressed in this article.

Simulations allow one to take into account non - linear effects and stochastic distributions and thus a more detailed modeling than analytical calculations. Simulations are therefore instrumental to improve the precision of the measurements and their interpretations. At least most of the principle techniques of data analysis using simulations are similar to those that have been invoked before. E.g. it was a standard method in analytical χ^2 minimizations to vary parameters in a model and see which one fits best. Simulations allow one to account for also subtle effects and many parameter variations with detailed templates. While such parameter variations motivate some philosophical literature to consider simulation as an 'experiment' by itself [20] they are no new quality of scientific practice¹³.

The higher precision comes at the price of higher complexity which naturally reflects itself in the complexity of validation. Required is the validation of each model in the chain since incorrectness of one of the models implies the whole simulation to be incorrect. Since simulation is factorizable, the complexity of validation is broken down into the validation of many 'simple' models. To the extent that the factorization is exhaustive and each factor is validated, the complete simulation is validated.

The models applied used have different confirmation statuses. Most of these are embedded in well established scientific practices that have grown and been confirmed over decades. Once such models have attained a very high level of confirmation, they acquire an almost autonomous status in simulation, i.e. their predictions are largely accepted. Other models are less certain, calling for more detailed scrutiny. E.g. simulation of the detector response for electrons is significantly better known than the emergence of jets from partons. Such

¹³New potentials through simulations may have been opened for using machine learning techniques in data analysis.

models are less trusted and call for specific care in validation.

However, even if models are strongly confirmed, there is a reluctance among particle physicists to rely too strongly on these. For once all models assume certain parametrizations and parameter values and it may depend on special circumstances if these are applicable. E.g. even though the interactions of an electron in a material are well known, the distribution of the material may be not. Therefore, in - situ validations or data driven methods are used to a large part. As discussed in this article, the individual model predictions at the LHC can be tested directly with complementary processes without any circular argumentation and are rather tightly constrained by the data. This appears to be in contrast to the claim of Morrison (cp.Sect. 6). In all these cases simulation is adjusted to describe the data - not vice versa, pointing to very different epistemic statuses of data and simulation.

Validation, however, has to account for the obvious fact that simulations cannot describe phenomena in all fine details. There is no validation 'per se' but only a validation with some uncertainty - validation in particle physics has to be quantifiable, leading to a systematic uncertainty of the simulation, which is a systematic uncertainty of the understanding of the measurement. At the LHC validation of the simulation and assigning a systematic uncertainty is almost synonymous and most of the work in LHC's data analysis is devoted to estimating these uncertainties. For some processes at the LHC the systematic uncertainty is reduced to the 0.1% level, for some they are much higher.

11 Summary and Conclusion

Simulation in particle physics is performed in factorizable steps that can be interpreted as migrating a 'true' distribution of an underlying parton process to the measurable one. This factorization allows one to validate the individual steps using specific measurements in which these steps are isolated and circularity with the target physics process is avoided.

In the validation process several models of different confirmation status are used. Some have been found to agree with data in many different experiments in the past, others are relatively new. This confirmation status affects how these models are applied, respectively which uncertainties are assigned. In all cases, particle physicists take pain to validate the models and their application using data, trying to minimize the reliance of simulation and its validation on models. One can distinguish the following methods:

- in - situ calibration of detector and physics processes,
- adopting previous precision measurements as references,
- deriving models from previous measurements and applying them to LHC data.

These different methods rely on data and models at different levels, also implying different ways to estimate the uncertainties.

In conclusion, substantial effort in particle physics is devoted to the validation of event simulation. The validation is in all steps significantly constraint by data. Models as autonomous entities are only invoked if they have been strongly confirmed in previous measurements. However, even in this case, the simulation is checked in an actual experiment. A quantitative estimate of the validity of the simulation is based on the factorization of individual contributions. Highly efficient methods have been devised to estimate and minimize the uncertainties with a strong effort to constrain those from data - either directly or reducing model choices.

Acknowledgement I am grateful to Martin King and Michael Stöltzner and anonymous referees for valuable comments. I also profited highly from discussions with colleagues from the Research Group 'Epistemology of the LHC' funded by the DFG under grant FOR 2063.

References

- [1] See e.g. C.Quigg, *Gauge Theories of the Strong, Weak, and Electromagnetic Interactions*, Princeton University Press, 2013
A.Pich, *The Standard Model of Electroweak Interactions*, in CERN Yellow Report CERN-2012-001, arXiv:1201.0537
- [2] C. Patrignani et al. (Particle Data Group), *Chin. Phys. C*, 40, 100001 (2016) and 2017 update.
- [3] L. Evans, (ed.), P. Bryant, (ed.), *LHC Machine*, JINST 3 (2008) S08001.
- [4] e.g. G.Gelmini, *TASI 2014 Lectures: the Hunt for Dark Matter*, arXiv:1502.01320v1 (2015)
- [5] e.g. Planck Collaboration (P.A.R. Ade et al.), *Planck 2015 results. XIV. Dark energy and modified gravity*, *Astron.Astrophys.* 594 (2016) A14, arXiv:1502.01590 (2015).
- [6] ATLAS Collaboration, *The ATLAS Experiment at the CERN Large Hadron Collider*, JINST 3, S08003 (2008).
- [7] CMS Collaboration, *The CMS experiment at the CERN LHC* JINST 3 (2008) S08004.
- [8] ALICE Collaboration, *The ALICE experiment at the CERN LHC*, JINST 3 (2008) S08002.
- [9] LHCb Collaboration, *The LHCb experiment at the CERN LHC*, JINST 3 (2008) S08005.
- [10] ATLAS Collaboration, <http://cds.cern.ch/record/1697048>
- [11] Gavin P. Salam, *Elements of QCD for hadron colliders*, in CERN Yellow Report CERN-2010-002, 45-100, arXiv:1011.5131
- [12] Michael H. Seymour, *Quantum ChromoDynamics*, Lectures given at the 2004 European School of High-Energy Physics, St. Feliu de Guixols, Barcelona, Spain, 30 May-12 June 2004 and at the 2009 Latin American School of High-Energy Physics, Recinto Quirama, Antioquia, Colombia, 15-28 March 2009, CERN-2006-003 and pp. 97-143 of CERN-2010-001 arXiv:hep-ph/0505192.
- [13] T.Gleisberg et al., *Event generation with SHERPA 1.1* JHEP, 02, 2009, 007, arXiv:0811.4622
- [14] ATLAS Collaboration, An computer generated image representing how ATLAS detects particles <https://cds.cern.ch/record/1505342>.
- [15] V. Daniel Elvira, *Impact of detector simulation in particle physics collider experiments* Phys.Rept. 695 (2017) 1, arXiv:1706.04293
- [16] GEANT4 Collaboration, S. Agostinelli et al., *Geant4 - a simulation toolkit* Nucl. Instrum. Meth. A 506, 250-303 (2003).
- [17] R. Ford, W. Nelson, *The EGS Code System - Version 3*, Stanford Linear Accelerator Center Report SLAC-210 (1978).
- [18] A. Ferrari, P. Sala, A. Fasso, , J. Ranft, *FLUKA: a multi-particle transport code*, CERN-2005-10 (2005), INFN/TC 05/11, SLAC-R-773.
- [19] ATLAS Collaboration, *A study of the material in the ATLAS inner detector using secondary hadronic interactions*, JINST 7 (2012) P01013, arXiv:1110.6191
- [20] E.Winsberg, *Computer Simulations in Science*, in Stanford Encyclopedia of Philosophy (2015)
- [21] M.Morrison, *Reconstructing Reality*, Oxford University Press (2015)
- [22] P.Mättig, *The Structure of Jets in $+e^-$ Collisions*, Phys.Rept. 177 (1989) 141.

- [23] I.G. Knowles and G.D. Lafferty, *Hadronization in Z^0 decay*, J.Phys. G23 (1997) 731, hep-ph/9705217
- [24] ATLAS Collaboration, *ATLAS measurements of the properties of jets for boosted particle searches*, Phys. Rev. D 86 (2012) 072006, arXiv:1206.5369
- [25] A.W.Campbell, J.W.Huston, W.J.Stirling, *Hard Interactions of Quarks and Gluons: A Primer for LHC Physics*, Rept.Prog.Phys. 70 (2007) 89, arXiv:hep-ph/0611148.
- [26] J.Butterworth et al., *PDF4LHC recommendations for LHC Run II*, J.Phys. G43 (2016) 023001, arXiv:1510.03865.
- [27] ATLAS Collaboration, *A Precision measurement and interpretation of inclusive W^+ , W^- and Z/γ production cross sections with the ATLAS detector*, Eur. Phys. J. C 77 (2017) 367, arXiv:1612.03016
- [28] ATLAS Collaboration, *Measurements of top-quark pair to Z-boson cross-section ratios at $\sqrt{s} = 13, 8, 7$ TeV with the ATLAS detector*, JHEP 02 (2017) 117, arXiv:1612.03636
- [29] ATLAS Collaboration, *Charged-particle distributions in $\sqrt{s} = 13$ TeV pp interactions measured with the ATLAS detector at the LHC*, j.physletb.2016.04.050, arXiv:1602.01633]
- [30] ALEPH and DELPHI and L3 and OPAL and SLD Collaborations and LEP Electroweak Working Group and SLD Electroweak Group and SLD Heavy Flavour Group (S. Schael et al.), *Precision electroweak measurements on the Z resonance*, Phys.Rept. 427 (2006) 257, hep-ex/0509008.
- [31] ATLAS Collaboration, *Measurement of the transverse momentum and ϕ_n^* distributions of Drell–Yan lepton pairs in proton-proton collisions at $\sqrt{s} = 8$ TeV with the ATLAS detector* Eur. Phys. J. C 76(5), 1-61 (2016), arXiv:1512.02192.
- [32] ATLAS Collaboration, *Electron and photon energy calibration with the ATLAS detector using LHC Run 1 data*, Eur. Phys. J. C (2014) 74: 3071, arXiv:1407.5063
- [33] ATLAS Collaboration, *Electron efficiency measurements with the ATLAS detector using 2012 LHC proton-proton collision data*, Eur. Phys. J. C 77 (2017) 195, arXiv:1612.01456
- [34] ATLAS Collaboration, *Muon reconstruction efficiency and momentum resolution of the ATLAS experiment in proton-proton collisions at $\sqrt{s} = 7$ TeV in 2010*, Eur.Phys.J. C74 (2014) no.9, 3034, arXiv:1404.4562.
- [35] ATLAS Collaboration, *Jet energy measurement and its systematic uncertainty in proton–proton collisions at $\sqrt{s} = 7$ TeV* Eur. Phys. J. C (2015) 75:17, arXiv:1406.0076
- [36] ATLAS Collaboration, *Observation of a New Particle in the Search for the Standard Model Higgs Boson with the ATLAS Detector at the LHC*, Phys. Lett. B 716 (2012) 1, arXiv:1207.7214
CMS Collaboration, *Observation of a new boson at a mass of 125 GeV with the CMS experiment at the LHC*, Phys. Lett. B 716 (2012) 30, arXiv:1207.7235
- [37] LHC Higgs Cross Section Working Group, S. Heinemeyer, C. Mariotti, G. Passarino and R. Tanaka (Eds.), *Handbook of LHC Higgs Cross Sections: 3. Higgs Properties*, CERN-2013-004 (CERN, Geneva, 2013), arXiv: 1307.1347 [hep-ph].
- [38] ATLAS Collaboration, *Measurement of the Higgs boson coupling properties in the $H \rightarrow ZZ^* \rightarrow 4l$ decay channel at $\sqrt{s} = 13$ TeV with the ATLAS detector*, JHEP 03 (2018) 095, arXiv: 1712.02304
- [39] ATLAS Collaboration, *Search for top squarks in final states with one isolated lepton, jets, and missing transverse momentum using 36.1fb^{-1} of $\sqrt{13}$ TeV pp collision data with the ATLAS detector*, submitted to JHEP, arXiv:1711.11520.